

University of Nebraska - Lincoln

DigitalCommons@University of Nebraska - Lincoln

---

Norman R. Simon Papers

Research Papers in Physics and Astronomy

---

1-1969

## Pulsational Instabilities in Hydrogen-Poor Massive Blue Stars

Norman R. Simon

University of Nebraska - Lincoln, [nsimon@unl.edu](mailto:nsimon@unl.edu)

Follow this and additional works at: <https://digitalcommons.unl.edu/physicssimon>

---

Simon, Norman R., "Pulsational Instabilities in Hydrogen-Poor Massive Blue Stars" (1969). *Norman R. Simon Papers*. 8.

<https://digitalcommons.unl.edu/physicssimon/8>

This Article is brought to you for free and open access by the Research Papers in Physics and Astronomy at DigitalCommons@University of Nebraska - Lincoln. It has been accepted for inclusion in Norman R. Simon Papers by an authorized administrator of DigitalCommons@University of Nebraska - Lincoln.

# PULSATIONAL INSTABILITIES IN HYDROGEN-POOR MASSIVE BLUE STARS. I

NORMAN R. SIMON AND RICHARD STOTHERS

Institute for Space Studies, Goddard Space Flight Center, NASA, New York

*Received May 13, 1968*

## ABSTRACT

The structure and pulsational properties of massive stars with helium cores and thin, hydrogen-poor envelopes have been investigated. The core structures are very insensitive to modifications of the hydrogen envelope. However, it is found that the total stellar radius and luminosity are modified by the integrated hydrogen content and by the hydrogen gradient, respectively. The models are pulsationally stable under modest conditions of central condensation (due to a hydrogen-burning shell and/or high hydrogen content). The unstable models are energized almost entirely by the helium reactions in the core, while most of the damping occurs in the thin hydrogen envelope. For each mass, the period is remarkably insensitive to the envelope modifications. The critical models dividing stable from unstable models are determined by (1) a pulsational eigenfrequency  $\omega^2 \sim 3$  and (2) the size of the hydrogen gradient. Our critical models explain some of the observed features of the classical Wolf-Rayet stars of high luminosity but seem to be too blue with respect to Rublev's sequence of stars on the H-R diagram.

## I. INTRODUCTION

Massive stars on the main sequence become unstable against nuclear-energized pulsations above a certain critical mass (Ledoux 1941; Schwarzschild and Härm 1959). However, evolution off the main sequence quickly stabilizes stars up to the greatest masses (Schwarzschild and Härm 1959). Even when the energy source shifts to a shell outside the contracted helium core, blue stars persist in exhibiting high pulsational stability (Ledoux 1941; Cox 1955; Stothers and Simon 1968). The relevant physical arguments have been amply reviewed in the foregoing references.

Most calculations of models so far have been based on the assumption that the stars evolve at constant mass and with developing chemical inhomogeneity. When either or both of these assumptions are relaxed, pulsational instability becomes a greater possibility. As a trivial formal example, consider the evolution of a completely mixed star during hydrogen burning. As hydrogen is depleted throughout the star, the critical mass for instability decreases as the inverse square of the mean molecular weight (Schwarzschild and Härm 1959):

$$M_{\text{crit}}/M_{\odot} = 21 \mu^{-2}.$$

A combination of somewhat more complex factors may result in more physically realistic examples. It is therefore of interest to ask what observational evidence exists for stars of high mass and blue color (because of the necessarily small central condensation) showing a significant degree of instability. The classical Wolf-Rayet stars are certainly prime candidates. However, their evolutionary stage is still a mystery and has been the subject of much discussion.

Among the more noteworthy proposals are the following. *Pre-main sequence*: gravitationally contracting stars (Sahade 1962; Underhill 1966). *Main sequence*: stars at the end of hydrogen burning (Westerlund 1961, 1964); stars having completely mixed at the end of hydrogen burning and now undergoing substantial loss of mass (Westerlund and Smith 1964); pulsationally unstable stars in secondary contraction at the end of hydrogen burning, in analogy with the  $\beta$  Cep stars (Stothers 1965). *Post-main sequence*: stars

evolved beyond hydrogen burning with substantial loss of mass (Limber 1964; Rublev 1965; Tanaka 1966; Paczynski 1967); stars that have completely mixed before, during, or after helium burning (cf. Burbidge *et al.* 1957); and stars in the helium-burning stage (Crawford 1953; Salpeter 1953; Divine 1965; Snezhko 1968). Clearly, virtually every possible evolutionary stage has been suggested!

In the present paper, we propose to study the structure and pulsational properties of post-main-sequence stars with massive helium cores and thin, hydrogen-poor envelopes. Pulsational instability (energized by nuclear reactions) may account for the observed variations in many W-R stars. The very high luminosities of some of the stars are assumed in the present work to be the consequence of high mass. Nevertheless, the original masses must have been still greater in order for the stars to have attained the assumed configurations.

## II. ASSUMPTIONS

The stellar models under consideration contain three zones: (1) a radiative outer zone with a smooth gradient of hydrogen and helium extending from the surface down to a thin shell (where hydrogen may or may not be burning); (2) a radiative intermediate zone, devoid of hydrogen, below the shell; and (3) a convective core where helium burning occurs.

The hydrogen abundance in the radiative outer zone is assumed to be a linear function of mass fraction

$$X = a_0 + a_1 q, \quad (1)$$

where  $a_0$  and  $a_1$  are determined by fixing the hydrogen content  $X_R$  at the surface ( $q = 1$ ) and requiring that  $X_s = 0.03$  at the shell ( $q_s$ ). The shell is approximated by a discontinuous jump in hydrogen and helium content as well as in luminosity. For simplicity, we shall consider only the initial model of helium burning in the core, so that the helium abundance below the shell may be represented by  $Y = 1 - Z$ , where  $Z$  is the zero-age metals abundance. Deinzer and Salpeter (1964) and Boury and Ledoux (1965) have shown that, in the case of stars composed of pure helium, little change in the structure and pulsational properties takes place as helium is depleted in the core. On this basis we assume that our results would not be altered much by the choice of a more evolved core. The metals abundance is taken to be  $Z = 0.03$  throughout our models.

The assumptions adopted here are similar to the ones adopted by Stothers (1966a) and by Stothers and Simon (1968), except that the present models lack a zone of zero-age chemical composition capping the zone of changing composition. The opacity is assumed to be due solely to electron scattering:

$$\kappa = 0.19(1 + X). \quad (2)$$

The nuclear-energy release is provided by the CNO cycle in the shell and by the triple-alpha reaction in the core. The rate of the former is given by

$$\epsilon_H = \epsilon_H^0 X X_{\text{CNO}} \rho T^{\nu_H}, \quad (3)$$

with

$$X_{\text{CNO}} = Z/2, \quad \nu_H = 14, \quad \log \epsilon_H^0 = -99.0$$

while the rate of the latter is given by

$$\epsilon_{\text{He}} = \epsilon_{\text{He}}^0 Y^3 \rho^2 T^{\nu_{\text{He}}}. \quad (4)$$

The quantities  $\epsilon_{\text{He}}^0$  and  $\nu_{\text{He}}$  are allowed to vary from model to model, since they are strongly dependent on temperature (Reeves 1965).

## III. STABLE MODELS

The masses selected for calculation are 15, 60, and 100  $M_{\odot}$ . The other free parameters which have to be specified for  $X_R$  and  $q_s$ .<sup>1</sup> The method of calculation has been described in Stothers (1966a). Results for each mass, using a variety of envelope parameters, are given in Table 1.

For a given mass, it is found that the luminosity remains approximately constant, while the spatial distribution of matter in the star (indicated by the stellar radius or by the radial extension of the shell) varies with the positioning of the shell in mass fraction  $q_s$  and with the surface abundance of hydrogen  $X_R$ . For increasingly homogeneous models ( $q_s \rightarrow 1$ ), both the total luminosity and the fraction of luminosity contributed by hydrogen burning decrease. Furthermore, the radius fraction of the shell increases with  $q_s$ , while the total radius decreases. Similar results were found by Cox and Salpeter (1961), Giannone (1967), Giannone, Kohl, and Weigert (1968), and Snezhko (1968) for models of stars with lower masses.

It is useful to differentiate two ways of formally altering the hydrogen content in the envelope: (1) addition of hydrogen, holding the mass fraction of the shell fixed; and (2) reduction of the mass fraction of the shell, holding the hydrogen abundance at the surface fixed. In both cases, the *integrated hydrogen content*  $\int X dq$  is increased, and so is the stellar *radius*. However, the *hydrogen gradient*  $dX/dq$  is steepened in case (1) and reduced in case (2); the stellar *luminosity* (as well as the hydrogen-burning fraction of the luminosity) decreases in case (1) and increases in case (2).

For models with a fixed core mass, alterations of the envelope composition have virtually no effect on the structure of the core. Thus, the core is effectively "decoupled" from the envelope and behaves like a single star (cf. Hayashi, Hōshi, and Sugimoto 1962).

A comparison of the various masses having the same envelope parameters ( $X_R$ ,  $q_s$ ) shows that the fraction of luminosity contributed by hydrogen burning is smaller at the higher masses. Depending on the selected envelope parameters (particularly  $q_s$ ), this fraction varies from less than 1 per cent to nearly 40 per cent in our models. However, for any constant set of envelope parameters, the basic stellar quantities show the same trends with mass as do normal main-sequence stars.

On account of the small amount of mass contained in the hydrogen envelopes, our models lie considerably to the left of the main sequence for stars burning hydrogen in the core (Stothers 1966b), although, of course, not as far left as the analogous main sequence for pure-helium stars (Deinzer and Salpeter 1964). Increasing the mass of the hydrogen envelopes still further can result in location of the models in the blue-supergiant region or even the red-supergiant region (Stothers and Chin 1968; Stothers and Simon 1968).

## IV. PULSATING MODELS

The radial pulsation characteristics of our models were calculated in the usual linear, quasi-adiabatic approximation (Schwarzschild and Härm 1959; Boury and Ledoux 1965; Stothers and Simon 1968). The relative pulsation amplitudes are all continuous through the star, except for the luminosity perturbation which has a discontinuity at the hydrogen shell. The average rate at which energy is being fed into, or removed from, the pulsations over a period is given by

$$L_P = L_{PN} - L_{PH} - L_{PS}, \quad (5)$$

<sup>1</sup> These depend on the previous evolution. If the star loses mass quickly at the end of core-hydrogen burning, as in a binary mass exchange, the hydrogen *gradient* remains unaltered, since it depends only on the initial hydrogen abundance,  $dX/dq \approx 1 + X_e$  (Stothers 1966b). With  $X_e = 0.70$ , our present models would have  $X_R \approx X_e + 1.7(1 - q_s)$ . However, we wish to be more general, allowing for more gradual mass loss, and therefore we allow  $X_R$  and  $q_s$  to be unrelated free parameters.

TABLE 1

MODEL CHARACTERISTICS FOR HELIUM-BURNING STARS WITH HYDROGEN-POOR ENVELOPES

	$M=15 M_{\odot}$				$M=60 M_{\odot}$						$M=100 M_{\odot}$					
$X_{R...}$	+ 0.10	+ 0.10	+ 0.05	+ 0.05	+ 0.15	+ 0.15	+ 0.15	+ 0.10	+ 0.05	+ 0.05	+ 0.15	+ 0.15	+ 0.10	+ 0.10	+ 0.05	+ 0.05
$q_s...$	+ 0.95	+ 0.98	+ 0.95	+ 0.97	+ 0.80	+ 0.95	+ 0.98	+ 0.95	+ 0.90	+ 0.95	+ 0.95	+ 0.97	+ 0.90	+ 0.95	+ 0.90	+ 0.93
$\beta_s...$	+ 0.681	+ 0.708	+ 0.680	+ 0.712	+ 0.200	+ 0.372	+ 0.388	+ 0.368	+ 0.247	+ 0.374	+ 0.289	+ 0.298	+ 0.197	+ 0.291	+ 0.189	+ 0.237
$\log T_s...$	+ 7.651	+ 7.518	+ 7.654	+ 7.577	+ 7.751	+ 7.685	+ 7.557	+ 7.689	+ 7.743	+ 7.695	+ 7.691	+ 7.620	+ 7.742	+ 7.698	+ 7.748	+ 7.732
$\log \rho_s...$	+ 0.876	+ 0.532	+ 0.882	+ 0.715	+ 0.245	+ 0.421	+ 0.067	+ 0.426	+ 0.338	+ 0.453	+ 0.274	+ 0.080	+ 0.209	+ 0.300	+ 0.206	+ 0.283
$r_s/R...$	+ 0.563	+ 0.661	+ 0.590	+ 0.655	+ 0.125	+ 0.487	+ 0.589	+ 0.524	+ 0.332	+ 0.570	+ 0.463	+ 0.523	+ 0.287	+ 0.517	+ 0.340	+ 0.454
$q...$	+ 0.763	+ 0.786	+ 0.763	+ 0.785	+ 0.664	+ 0.879	+ 0.922	+ 0.876	+ 0.770	+ 0.879	+ 0.894	+ 0.924	+ 0.796	+ 0.895	+ 0.792	+ 0.842
$\beta_c...$	+ 0.592	+ 0.591	+ 0.592	+ 0.591	+ 0.372	+ 0.347	+ 0.347	+ 0.347	+ 0.354	+ 0.346	+ 0.279	+ 0.278	+ 0.284	+ 0.278	+ 0.284	+ 0.280
$\log T_c...$	+ 8.287	+ 8.287	+ 8.287	+ 8.287	+ 8.327	+ 8.333	+ 8.334	+ 8.333	+ 8.331	+ 8.333	+ 8.348	+ 8.349	+ 8.346	+ 8.348	+ 8.346	+ 8.347
$\log \rho_c...$	+ 2.637	+ 2.636	+ 2.637	+ 2.636	+ 2.368	+ 2.339	+ 2.340	+ 2.339	+ 2.346	+ 2.338	+ 2.245	+ 2.246	+ 2.251	+ 2.245	+ 2.249	+ 2.246
$\rho_c/\langle \rho \rangle$	+ 34.4	+ 27.7	+ 29.8	+ 25.0	+3560.0	+ 66.8	+ 50.8	+ 53.6	+201.0	+ 40.6	+ 83.7	+ 69.2	+329.0	+ 58.9	+196.0	+ 82.8
$L_H/L$	+ 0.089	+ 0.000	+ 0.110	+ 0.004	+ 0.377	+ 0.045	+ 0.000	+ 0.069	+ 0.299	+ 0.075	+ 0.033	+ 0.001	+ 0.222	+ 0.046	+ 0.245	+ 0.165
$\log (L/L_{\odot})...$	+ 5.471	+ 5.440	+ 5.481	+ 5.441	+ 6.411	+ 6.359	+ 6.355	+ 6.370	+ 6.438	+ 6.374	+ 6.636	+ 6.635	+ 6.680	+ 6.642	+ 6.692	+ 6.676
$\log (R/R_{\odot})...$	+ 0.075	+ 0.044	+ 0.054	+ 0.029	+ 1.037	+ 0.471	+ 0.431	+ 0.439	+ 0.628	+ 0.399	+ 0.609	+ 0.581	+ 0.805	+ 0.558	+ 0.731	+ 0.607
$\log T_e...$	+ 5.093	+ 5.101	+ 5.106	+ 5.109	+ 4.847	+ 5.118	+ 5.136	+ 5.136	+ 5.059	+ 5.157	+ 5.118	+ 5.131	+ 5.031	+ 5.145	+ 5.070	+ 5.129
$\nu_{He...}$	+ 20.0	+ 20.0	+ 20.0	+ 20.0	+ 18.0	+ 17.0	+ 17.0	+ 17.0	+ 18.0	+ 17.0	+ 17.0	+ 17.0	+ 17.0	+ 17.0	+ 17.0	+ 17.0
$\log \epsilon_{He^0...}$	-164.8	-164.8	-164.8	-164.8	- 148.2	-139.9	-139.9	-139.9	-148.2	-139.9	-139.9	-139.9	-139.9	-139.9	-139.9	-139.9

TABLE 2

PULSATATIONAL CHARACTERISTICS FOR MODELS OF TABLE 1

	$M=15 M_{\odot}$				$M=60 M_{\odot}$						$M=100 M_{\odot}$					
$X_R$	+0.10	+0.10	+0.05	+0.05	+ 0.15	+0.15	+0.15	+0.10	+ 0.05	+0.05	+0.15	+0.15	+0.10	+0.10	+ 0.05	+0.05
$q_s...$	+0.95	+0.98	+0.95	+0.97	+ 0.80	+0.95	+0.98	+0.95	+ 0.90	+0.95	+0.95	+0.97	+0.90	+0.95	+ 0.90	+0.93
$\omega^2$	+4.044	+3.403	+3.546	+3.076	+ 6.521	+3.505	+2.828	+2.866	+ 5.507	+2.235	+3.295	+2.847	+5.855	+2.401	+ 4.655	+3.015
Period (hr)	+0.46	+0.45	+0.46	+0.45	+ 5.07	+0.98	+0.95	+0.97	+ 1.34	+0.96	+1.26	+1.23	+1.86	+1.23	+ 1.61	+1.30
$\beta_R...$	+0.679	+0.701	+0.686	+0.713	+ 0.268	+0.350	+0.356	+0.363	+ 0.290	+0.386	+0.263	+0.265	+0.219	+0.285	+ 0.235	+0.262
$\log \rho_R...$	-7.149	-7.082	-7.064	-6.999	- 8.680	-7.700	-7.632	-7.590	- 7.936	-7.453	-7.879	-7.835	-8.215	-7.720	- 8.024	-7.785
$\log g_R...$	+5.464	+5.525	+5.505	+5.555	+ 4.140	+5.274	+5.353	+5.338	+ 4.959	+5.417	+5.219	+5.275	+4.826	+5.322	+ 4.974	+5.223
$(\delta r/r)_R...$	+1.000	+1.000	+1.000	+1.000	+ 1.000	+1.000	+1.000	+1.000	+ 1.000	+1.000	+1.000	+1.000	+1.000	+1.000	+ 1.000	+1.000
$(\delta T/T)_R...$	-2.205	-2.050	-2.075	-1.971	-2.652	-1.906	-1.735	-1.746	- 2.401	-1.590	-1.839	-1.726	-2.477	-1.616	- 2.178	-1.768
$(\delta L/L)_R...$	-4.280	-4.199	-4.300	-3.885	- 6.610	-3.624	-2.940	-2.985	- 5.603	-2.359	-3.354	-2.903	-5.908	-2.464	- 4.710	-3.071
$(\delta r/r)_s...$	+0.416	+0.566	+0.495	+0.606	+ 0.009	+0.369	+0.524	+0.480	+ 0.088	+0.608	+0.368	+0.465	+0.054	+0.533	+ 0.143	+0.394
$(\delta T/T)_s...$	-0.630	-0.887	-0.739	-0.921	- 0.014	-0.473	-0.682	-0.604	- 0.129	-0.751	-0.453	-0.576	-0.077	-0.642	- 0.193	-0.488
$(\delta L/L)_s...$	-0.510	-0.887	-0.607	-0.876	- 0.001	-0.186	-0.355	-0.245	- 0.026	-0.315	-0.140	-0.215	-0.010	-0.210	- 0.035	-0.134
$(\delta r/r)_c...$	+0.320	+0.422	+0.384	+0.467	+ 0.005	+0.301	+0.417	+0.395	+ 0.060	+0.508	+0.307	+0.384	+0.038	+0.452	+ 0.106	+0.323
$(\delta T/T)_c...$	-0.369	-0.486	-0.443	-0.539	- 0.006	-0.320	-0.443	-0.419	- 0.064	-0.539	-0.321	-0.402	-0.040	-0.473	- 0.111	-0.338
$L_{PN}^*/L...$	+0.69	0.00	+0.89	+0.06	0.00	+0.22	0.00	+0.37	+ 0.09	+0.63	+0.15	+0.01	+0.02	+0.36	+ 0.16	+0.62
$L_{PN}^c/L...$	+3.199	+6.085	+4.504	+7.448	0.000	+2.262	+4.487	+3.767	+ 0.069	+6.190	+2.282	+3.696	+0.03	+4.900	+ 0.213	+2.231
$L_{PN}/L...$	+3.89	+6.09	+5.40	+7.50	0.00	+2.48	+4.49	+4.13	+ 0.16	+6.82	+2.43	+3.71	+0.05	+5.27	+ 0.37	+2.85
$L_{PH}^c/L...$	+6.613	+5.416	+5.591	+4.843	+10.534	+4.482	+3.374	+3.462	+ 8.234	+2.538	+4.053	+3.349	+8.895	+2.721	+ 6.415	+3.609
$L_{PH}^c/L...$	+0.121	+0.219	+0.174	+0.269	0.000	+0.047	+0.113	+0.081	+ 0.001	-0.135	+0.037	+0.069	0.000	+0.081	+ 0.003	+0.033
$L_{PH}/L...$	+6.734	+5.636	+5.765	+5.112	+10.534	+4.530	+3.488	+3.542	+ 8.235	+2.672	+4.090	+3.418	+8.895	+2.802	+ 6.417	+3.641
$L_{PS}/L...$	+1.129	+1.105	+1.092	+1.122	+ 0.271	+0.511	+0.450	+0.474	+ 0.533	+0.439	+0.442	+0.403	+0.492	+0.391	+ 0.486	+0.431
$L_P/L...$	-3.97	-0.65	-1.46	-1.27	-10.80	-2.56	+0.55	+0.12	- 8.61	+3.71	-2.10	-0.12	-9.33	+2.07	- 6.53	-1.22
$L_P^*/L...$	-2.85	+0.45	-0.37	+2.39	-10.53	-2.04	+1.00	+0.59	- 8.08	+4.15	-1.66	+0.29	-8.84	+2.46	- 6.05	-0.79
$1/K$ (yr)	- 725	- 7860	- 2730	+4930	- 8.858	-488	+4170	+17400	-12.2	+885	-537	-14800	-5.69	+1440	-32.4	- 999
$1/K^*$ (yr)	-1010	+11300	-10100	+2620	- 0.880	-610	+2290	+ 3460	-13.0	+792	-680	+ 5930	-6.01	+ 957	-35.0	-1540

\* Indicates neglect of running waves.

1969ApJ...155..247S



where  $L_{PN}$  is the rate of gain from nuclear sources,  $L_{PH}$  is the rate of flux damping, and  $L_{PS}$  is the rate of damping by acoustical waves running off the surface. A positive sign for  $L_P$  indicates an unstable configuration. The energizing term  $L_{PN}$  contains a contribution from both hydrogen burning in the shell,  $L_{PN}^s$ , and helium burning in the core,  $L_{PN}^c$  while the main damping term  $L_{PH}$  is the sum of the rates of heat loss in the envelope  $L_{PH}^e$  and in the convective core  $L_{PH}^c$ . To avoid the difficulty involved in calculating luminosity amplitudes in a convective region (cf. Boursy, Gabriel, and Ledoux 1964), we have estimated them following Schwarzschild and Härm (1959) by means of an average involving quantities computed at the center and the outer boundary of the core only. Such an approximation is sufficient for our purpose because the contribution from these terms is small, never exceeding 30 per cent of the contribution from the surface waves.

The calculated pulsational rates are listed in Table 2, along with the square of the dimensionless frequency

$$\omega^2 = \left( \frac{2\pi}{\text{Period}} \right)^2 \frac{R^3}{GM}; \quad (6)$$

the pulsational  $e$ -folding time  $1/K$ , where  $K$  is the stability coefficient ( $L_P/2E_P$ ) and  $E_P$  is the mechanical energy of the pulsations; and the relative pulsation amplitudes at the surface, shell, and center. The quantities with asterisks have been computed without the contribution from surface waves. Otherwise, the notation is the same as in previous papers (Schwarzschild and Härm 1959; Stothers and Simon 1968).

The general conclusions that can be drawn regarding the pulsational eigenfrequencies are already known. For example,  $\omega^2$  increases with greater central condensation (as measured by  $\rho_c/\langle\rho\rangle$ ) and decreases with greater relative radiation pressure (as measured by  $1 - \beta_c$ ). For reference, we note (1) a greater central condensation with increasing radius and (2) a greater relative radiation pressure with increasing luminosity and hence with increasing mass. The critical value of  $\omega^2$  dividing the stable and unstable models is approximately the same for all masses ( $\omega^2 \sim 3$ ). The reason is that the critical central condensation increases along with the relative radiation pressure at higher masses (see below and Appendix). This result for the critical value of  $\omega^2$  seems to be valid not only for our hybrid models but also for pure-helium stars (Boursy and Ledoux 1965) and for Population I hydrogen main-sequence stars (Schwarzschild and Härm 1959).

The pulsation periods of those four models lying in the vicinity of the critical model for each mass are remarkably similar. This result is surprising in view of the fact that the integrated hydrogen abundance and the hydrogen gradient vary by factors up to 6 and 8, respectively. The increase of  $\omega^2$  with radius is apparently such that the period is held nearly constant (eq. [6]).

In all the models, most of the damping comes from heat leakage in the envelope. The core contributes less than 5 per cent of the interior damping, and the surface waves contribute less than 20 per cent of the total damping (interior plus surface). Energizing of the pulsations comes almost entirely from the helium reactions in the core. The hydrogen shell contributes less than 10 per cent of the energy for pulsations in all the unstable models. This is in general due to the fact that  $L_H/L$  is small in the unstable models, although the smallness of  $L_H/L$  is not a sufficient condition for instability. When the shell is vigorously burning and/or hydrogen is added to the envelope, the envelope is in an expanded state. Such an expansion drives up the central condensation because the central density is fixed at a nearly constant value by the helium-burning reactions. Consequently, the pulsation amplitudes drop off more rapidly inside the surface (see Appendix) and therefore are smaller near the center where most of the destabilization takes place. Hence, a high central condensation tends to induce stability. The critical value of  $\rho_c/\langle\rho\rangle$  dividing the stable and unstable models for each mass is given in Table 3. The corresponding value of  $\delta r/r$  at the center is about 40 per cent of the surface amplitude in all cases.

In Table 3 we have also listed the critical value of  $q_s$  for each selected mass and surface abundance of hydrogen. An asterisk again indicates that surface waves have been neglected. In general, the deeper the mass fraction of the shell, the less surface abundance of hydrogen is required to induce stability. The key factor determining the critical model for a given mass seems to be the *hydrogen gradient* rather than merely the total amount of hydrogen. This is so since the hydrogen gradient is a more delicate regulator of the degree of central condensation. On account of the smaller radiation pressure at lower mass, the low-mass models become unstable under more restrictive conditions on the hydrogen gradient. In the limit of vanishing hydrogen content (pure-helium stars) the critical mass is 7–8  $M_\odot$  (Boury and Ledoux 1965).

TABLE 3  
CRITICAL MODELS DIVIDING STABLE FROM UNSTABLE MODELS

	7–8 $M_\odot$	15 $M_\odot$		60 $M_\odot$			100 $M_\odot$		
$X_R \dots$	. . .	0 10	0 05	0 15	0 10	0.05	0 15	0.10	0.05
$q_s$	1 00	0 98	0 96	0 98	0 95	0 94	0 97	0 94	0 94
$q_s^*$	1.00	0 98	0 95	0 97	0 94	0 93	0.97	0 94	0 93
$\omega^2 \dots$	3 6	3.3		2 9			2.8		
Period (hr) ..	0 30	0 45		0.97			1 23		
$\rho_c / \langle \rho \rangle \dots$	20	27		54			69		

\* Indicates neglect of running waves.

V. COMPARISON WITH OBSERVATIONS

The location of Wolf-Rayet stars on the H-R diagram is very uncertain, and there is much confusion and argument concerning where they lie with respect to the main sequence. This is true as regards both luminosity and effective temperature. In addition, the masses of these stars are not well known. There are, however, some generally agreed-upon properties of Wolf-Rayet stars which are of interest here, although they will be discussed in more detail in a subsequent paper.

First of all, the classical W-R stars are rare objects and must be young because of their close association with O and B stars. Second, these objects seem to be superluminous (as compared with main-sequence stars) for any reasonable masses that are assigned them. Third, many of the stars are surrounded by expanding shells and sometimes by large, dense nebulae. Fourth, their emission lines are frequently observed to vary irregularly on a time scale of hours. Fifth, their electron temperatures are very high, and their effective temperatures may also be very hot (possibly hotter than main-sequence stars). Sixth, the atmospheres of these stars seem to be rich in helium and, in the case of the WN sequence, possibly rich in nitrogen as well (as if the surface material had at one time been processed through the CN cycle).

It has often been suggested in the literature that W-R stars may arise as a result of mass loss. Rublev (1965) states: "It cannot be excluded that WR stars are some sort of remnants of initially very massive stars that have shed a considerable portion of their matter (including all of the hydrogen-rich envelope) and have uncovered layers which during the earlier stages of evolution corresponded to the periphery of the convective core."

The foregoing evidence allows us to make the tentative suggestion that some W-R stars may be massive objects in the stage of evolution where helium is burned in the

core and, further, that the structure of these stars could be approximated by our hydrogen-poor, helium-burning models.

Let us examine this suggestion. Figure 1 shows a plot of the H-R diagram of our model stars (open circles), including pulsationally unstable models (crossed open circles). The filled circles represent W-R stars as located by Rublev (1965). The pure-helium sequence (Deinzer and Salpeter 1964) and the normal main sequence (Stothers 1966*b*) along with approximate mass locations are drawn in for reference at left and at right, respectively.

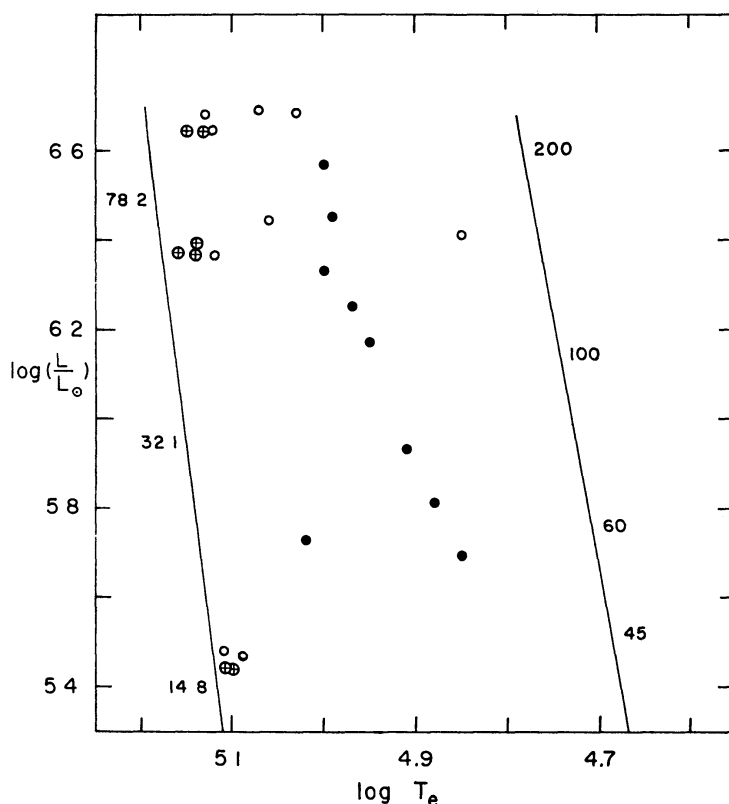


FIG. 1.—Theoretical H-R diagram for superluminous massive stars. *Filled circles*, W-R stars as located by Rublev. *Open circles*, our models, including unstable models (*crossed open circles*). The stars are bounded on the left and right by the pure-helium sequence and normal main sequence, respectively; several masses (solar units) are indicated.

It is immediately clear that all W-R stars on the diagram are superluminous, the least luminous star corresponding to a main-sequence mass of about  $60 M_{\odot}$ . This suggests that the W-R stars are not hydrogen-burning stars, but represent rather a post-main-sequence phase of evolution. If such an evolutionary stage is indeed reached via mass loss on the upper main sequence, then the expanding shells and nebulae which surround Wolf-Rayet stars may be attributed to the ejected matter.

As previously noted, W-R masses are extremely uncertain. Underhill (1966) estimates the average mass in binary systems to lie between 4 and  $8 M_{\odot}$ , while, if one takes Rublev's stars to be burning core helium, his highest mass appears to be  $\sim 90 M_{\odot}$ .

Let us turn now to the question of W-R stability. As can be seen in Figure 1, a narrow band of instability exists for our hydrogen-poor models, running close to the pure-helium sequence and turning off slightly at high masses. Since Rublev's estimates of



effective temperature are higher than most quoted in the literature, it seems unlikely (though still possible) that the W-R locus can be moved any farther to the left. In that case, pulsations energized by a helium core cannot be the cause of observed variability, since the cooler of our models prove to be quite stable.

It is clear that any mechanism which will account for the present observed properties of luminous W-R stars should also fit in with the previous evolutionary history of mass loss. In a forthcoming paper, we shall propose just such a unified mechanism.

One of us (N. R. S.) gratefully acknowledges the support of a Yeshiva University fellowship during the academic year 1966–1967, and of a NAS-NRC Research Associateship under the National Aeronautics and Space Administration.

# APPENDIX

It is required to show that the gradient of the radius amplitude at the surface is steeper for a higher central condensation. The relevant linearized equations for adiabatic pulsations are

$$\begin{aligned} x \frac{d}{dx} \left( \frac{\delta r}{r} \right) &= - \frac{\delta \rho}{\rho} - 3 \frac{\delta r}{r}, \\ x \frac{d}{dx} \left( \frac{\delta P}{P} \right) &= V \frac{\delta P}{P} + V \left( 4 + \omega^2 \frac{x^3}{q} \right) \frac{\delta r}{r}, \\ \frac{\delta P}{P} &= \Gamma \frac{\delta \rho}{\rho}, \quad \text{with} \quad \Gamma = \beta + \frac{2}{3} \frac{(4 - 3\beta)^2}{\beta + 8(1 - \beta)}. \end{aligned}$$

At the surface,  $x = 1$ ,  $q = 1$ , and  $V = -d \ln P / d \ln r = \infty$ . Therefore, we need the regularity condition

$$\left( \frac{\delta P}{P} \right)_R = - (4 + \omega^2) \left( \frac{\delta r}{r} \right)_R.$$

The gradient at the surface is clearly

$$\frac{d}{dx} \left( \frac{\delta r}{r} \right) = \frac{\omega^2 - (3\Gamma_R - 4)}{\Gamma_R},$$

setting  $(\delta r/r)_R = 1$ .

We now make use of the well-known variational result (Ledoux and Walraven 1958),

$$\omega^2 \leq (3\langle \Gamma \rangle - 4)J,$$

where the ratio

$$J = \int_0^1 \frac{q}{x} dq / \int_0^1 x^2 dq$$

is a measure of the central condensation, like  $\rho_c / \langle \rho \rangle$ . Clearly,  $\omega^2$  increases with increasing central condensation and with decreasing relative radiation pressure. As an approximation, we set  $\langle \Gamma \rangle = \Gamma_R$  and use the equality sign in the variational expression for  $\omega^2$ . Then

$$\frac{d}{dx} \left( \frac{\delta r}{r} \right) = \frac{3\Gamma_R - 4}{\Gamma_R} (J - 1).$$

At the stellar surface  $\Gamma_R$  is determined from

$$\beta_R = 1 - (\kappa_R L / 4\pi c G M).$$

For a given mass and chemical composition, the surface value of  $\beta$  and thus of  $\Gamma$  depends only on the luminosity. But the luminosity is not very sensitive to chemical composition of the envelope. Hence, for a given mass,

$$\frac{d}{dx} \left( \frac{\delta r}{r} \right) \sim J - 1.$$

This indicates the more rapid drop-off of pulsation amplitudes (all of which depend on  $\delta r/r$ ) with higher central condensation.

#### REFERENCES

- Boury, A., Gabriel, M., and Ledoux, P. 1964, *Ann. d'ap.*, **27**, 92.  
 Boury, A., and Ledoux, P. 1965, *Ann. d'ap.*, **28**, 353.  
 Burbidge, E. M., Burbidge, G. R., Fowler, W. A., and Hoyle, F. 1957, *Rev. Mod. Phys.*, **29**, 547.  
 Cox, J. P. 1955, *Ap. J.*, **122**, 286.  
 Cox, J. P., and Salpeter, E. E. 1961, *Ap. J.*, **133**, 764.  
 Crawford, J. A. 1953, *Pub. Astr. Soc. Pacific*, **65**, 210.  
 Deinzer, W., and Salpeter, E. E. 1964, *Ap. J.*, **140**, 499.  
 Divine, N. 1965, *Ap. J.*, **142**, 824.  
 Giannone, P. 1967, *Zs. f. Ap.*, **65**, 226.  
 Giannone, P., Kohl, K., and Weigert, A. 1968, *Zs. f. Ap.*, **68**, 107.  
 Hayashi, C., Hōshi, R., and Sugimoto, D. 1962, *Progr. Theoret. Phys. Suppl.* (Kyoto), No. 22.  
 Ledoux, P. 1941, *Ap. J.*, **94**, 537.  
 Ledoux, P., and Walraven, Th. 1958, in *Hdb. d. Phys.*, ed. S. Flügge (Berlin: Springer-Verlag), **51**, 353.  
 Limber, D. N. 1964, *Ap. J.*, **139**, 1251.  
 Paczynski, B. 1967, *Acta Astr.*, **17**, 355.  
 Reeves, H. 1965, in *Stellar Structure*, ed. L. H. Aller and D. B. McLaughlin (Chicago: University of Chicago Press), p. 113.  
 Rublev, S. V. 1965, *Astr. Zh.*, **42**, 347.  
 Sahade, J. 1962, *Symposium on Stellar Evolution* (La Plata, Argentina: National University of La Plata), p. 185.  
 Salpeter, E. E. 1953, *Ann. Rev. Nucl. Sci.*, **2**, 41.  
 Schwarzschild, M., and Härm, R. 1959, *Ap. J.*, **129**, 637.  
 Snezhko, L. I. 1968, *Astr. Zh.*, **45**, 251.  
 Stothers, R. 1965, *Ap. J.*, **141**, 671.  
 ———. 1966a, *ibid.*, **143**, 91.  
 ———. 1966b, *ibid.*, **144**, 959.  
 Stothers, R., and Chin, C.-w. 1968, *Ap. J.*, **152**, 225.  
 Stothers, R., and Simon, N. R. 1968, *Ap. J.*, **152**, 233.  
 Tanaka, Y. 1966, *Pub. Astr. Soc. Japan*, **18**, 47.  
 Underhill, A. B. 1966, *The Early Type Stars* (Dordrecht: D. Reidel Pub. Co.).  
 Westerlund, B. 1961, *Uppsala Ann.*, **5**, No. 1.  
 ———. 1964, in *The Galaxy and the Magellanic Clouds* (IAU/URSI Symp. No. 20), ed. F. J. Kerr and A. W. Rodgers (Canberra: Australian Academy of Science), p. 316.  
 Westerlund, B. E., and Smith, L. F. 1964, *M.N.R.A.S.*, **128**, 311.

Copyright 1969 The University of Chicago. Printed in U.S.A.

